Diagnostic performance of 68Ga-PSMA-PET/MRI versus 68Ga-PSMA-PET/CT in the evaluation of lymph node and bone metastases of prostate cancer

Martin Thomas Freitag[1], Jan Radtke[1,2], Boris Hadaschik[2], Uwe Haberkorn[3], Heinz-Peter Schlemmer[1], Matthias Roethke[1], and Ali Afshar-Oromieh[3]
[1]Department of Radiology, German Cancer Research Center, Heidelberg, Baden-Wuerttemberg, Germany, [2]Department of Urology, University hospital of Heidelberg, Heidelberg, Baden-Wuerttemberg, Germany, [3]Department of Nuclear Medicine, University hospital of Heidelberg, Heidelberg, Baden-Wuerttemberg, Germany

Purpose

The Prostate-specific membrane antigen (PSMA) is highly expressed in cells derived from prostate cancer[1]. Direct targeting of PSMA using a ^{68}Gallium-based ligand as well as the first application in a patient was described in 2012[1,2], followed by the first study demonstrating a systematic application in 2013[3]. The development of this novel tracer is regarded as a significant improvement for the diagnosis of prostate cancer. The positive predictive value of ^{68}Ga-PSMA-PET/CT was recently reported to be extremely high and thus, a PSMA-PET-positive finding is highly suggestible for prostate cancer or metastasis[4]. The next stage of development would involve the establishment of ^{68}Ga-PSMA-PET/MRI. A study reporting initial experience in the comparison of a hybrid PET/MRI versus PET/CT for PSMA-based examinations has discussed potential advantages of PET/MRI over PET/CT[5]. However, these advantages, such as the known high soft tissue contrast and the option for multiparametric assessments, were not analyzed in detail in the before-mentioned study. Here, we consider this multiparametric option of PET/MRI by including four different MR parameters and systematically compare the diagnostic performance of ^{68}Ga-PSMA-PET/MRI with ^{68}Ga-PSMA-PET/CT in lymph node (LN) and bone metastases of patients with a history of prostate cancer.

Materials and Methods

The study was conducted in accordance with the declaration of Helsinki including institutional approval by the local ethics committee. Twenty-six patients with recurrent prostate cancer were included. All patients underwent PET/CT 1h and PET/MRI 3h after injection of the PSMA-ligand ^{68}Ga-PSMA-11 (HBED-CC). PET/MRI sequences included T1w FLASH3D native and contrast-enhanced, T2w-fatsat (turbo-spin-echo) and diffusion-weighted sequences (b-values 50 and 800 s/mm^2). In every LN and bone lesion with focal PSMA-uptake, the conspicuity (0-3) of a morphological correlate was evaluated by two independent readers. This score served as a semi-quantitative measurement to reflect the intrinsic contrast-to-noise. The arithmetic mean between both readers was compared using Wilcoxon signed-rank test including Bonferroni-Holm correction. In PET-positive LNs and bone lesions, SUV values were quantified and correlated. The short axis diameters of PET-positive LNs were quantified to determine a potential pathological enlargement. Four discordant PET-positive findings (3 LNs, 1 bone lesion) were excluded from the study, 64 PET-positive LNs and 28 bone lesions were compared.

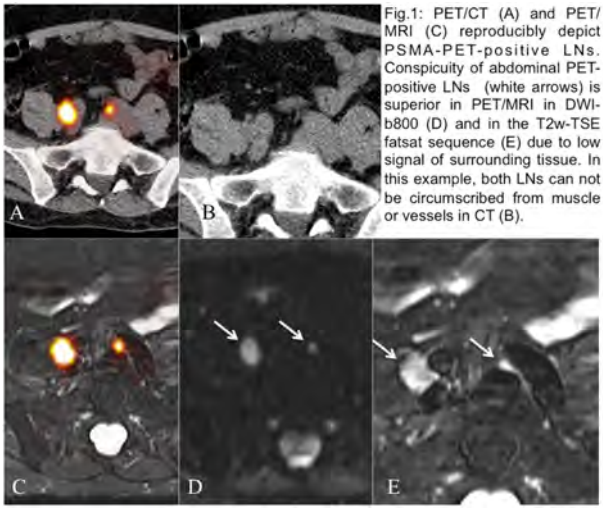

Fig.1: PET/CT (A) and PET/MRI (C) reproducibly depict PSMA-PET-positive LNs. Conspicuity of abdominal PET-positive LNs (white arrows) is superior in PET/MRI in DWI-b800 (D) and in the T2w-TSE fatsat sequence (E) due to low signal of surrounding tissue. In this example, both LNs can not be circumscribed from muscle or vessels in CT (B).

Results

We observed a significant linear correlation between both methods with regard to SUV values for 64 PET-positive LNs (ρ_{SUVmax}=0.89, p<0.0001; $\rho_{SUVmean}$=0.87, p<0.0001) and also for 28 osseous metastases (ρ_{SUVmax}=0.75, p<0.0001; $\rho_{SUVmean}$=0.72, p<0.0001). Conspicuity was significantly better in MRI for LNs using T1w-CE-fatsat (p=0.014), T2w-fatsat (p=0.0001) and DWI (p=0.0001) sequences compared to CT (Table 1, Figure 1). Remarkably, 73.4% (n=47) of PET-positive LNs were smaller than 1 cm in short axis diameter thus not appearing pathologically enlarged. For osseous metastases, there was no significantly increased lesion conspicuity observed for any of the employed MRI sequences but the highest MR score per lesion was significantly increased compared to CT.

Discussion

Our results indicate that PSMA-positive LNs and bone lesions are depicted reproducibly PET-positive in PET/MRI and PET/CT examinations. PET/MRI provides superior conspicuity of PET-positive LNs compared to PET/CT with best results for fat-saturated T2w TSE and diffusion weighted sequences due to strong suppression of signal from muscle, fat and vessels. This is useful in especially small LNs (73.4% of PET-positive LNs). For bone lesions, PET/MRI and PET/CT demonstrate similar potential although PET/MRI may be advantageous in individual patients as reflected by the highest MRI conspicuity score per lesion.

Conspicuity of LNs (n=64)	**CT**	**T1w**	**T2w TSE fatsat**	**T1w CE fatsat**	**DWI (b800)**	**highest MRI score/lesion**
Mean of both readers	2.34±0.71	2.45±0.63	2.78±0.33	2.53±0.56	2.88±0.30	2.95±0.20
MRI conspicuity higher than CT?	-	no (p=0.18, Z=-1.34)	**yes** (p<0.0001, Z=-4.80) [B]	**yes** (p=0.013, Z=-2.47) [B]	**yes** (p<0.0001, Z=-5.25) [B]	**yes** (p<0.0001, Z=-5.44) [B]
Conspicuity of bone lesions (n=28)	**CT**	**T1w**	**T2w TSE fatsat**	**T1w CE fatsat**	**DWI (b800)**	**highest MRI score/lesion**
Mean of both readers	2.39±1.04	2.41±0.68	2.75±0.44	2.57±0.56	2.73±0.67	2.96±0.13
MRI conspicuity higher than CT?	-	no (p=0.82, Z=-0.22)	no (p=0.15, Z=-1.43)	no (p=0.64, Z=-0.46)	no (p=0.19, Z=-1.31)	**yes** (p=0.006, Z=-2.73) [B]

Table 1: Lesion conspicuity. [B]: Bonferroni-Holm-corrected.

References: [1]Eder M et al., 2012; Bioconjug Chem. [2]Afshar-Oromieh et al., 2012; Eur J Nucl Med Mol Imaging [3]Afshar-Oromieh et al., 2013; Eur J Nucl Med Mol Imaging. [4]Afshar-Oromieh et al., 2014; accepted; Eur J Nucl Med Mol Imaging [5]Afshar-Oromieh et al., 2014; Eur J Nucl Med Mol Imaging.